Journal of Alloys and Compounds 508 (2010) 523–527

Contents lists available at ScienceDirect

Journal of Alloys and Compounds

journal homepage: www.elsevier.com/locate/jallcom

Mechanical properties of the hexagonal $HoMnO_3$ thin films by nanoindentation

Cheng-Yo Yen[a], Sheng-Rui Jian[a,*], Yi-Shao Lai[b], Ping-Feng Yang[b], Ying-Yen Liao[c], Jason Shian-Ching Jang[d], Tjung-Han Lin[e], Jenh-Yih Juang[e]

[a] Department of Materials Science and Engineering, I-Shou University, Kaohsiung 840, Taiwan
[b] Central Product Solutions, Advanced Semiconductor Engineering, Inc., 26 Chin 3rd Rd., Nantze Export Processing Zone, Kaohsiung 811, Taiwan
[c] Department of Applied Physics, National University of Kaohsiung, Kaohsiung 81148, Taiwan
[d] Department of Mechanical Engineering; Institute of Materials Science & Engineering, National Central University, Chung-Li 320, Taiwan
[e] Department of Electrophysics, National Chiao Tung University, Hsinchu 300, Taiwan

ARTICLE INFO

Article history:
Received 16 April 2010
Received in revised form 8 August 2010
Accepted 15 August 2010
Available online 19 September 2010

Keywords:
Hexagonal $HoMnO_3$ thin films
XRD
Nanoindentation
Hardness

ABSTRACT

The structural and nanomechanical characteristics of the hexagonal $HoMnO_3$ (HMO) thin films are investigated by means of X-ray diffraction (XRD), atomic force microscopy (AFM) and nanoindentation techniques in this study. The HMO thin films were deposited on YSZ(1 1 1) substrates by pulsed laser deposition (PLD). The XRD results reveal only pure (0 0 0 1)-oriented hexagonal HMO reflections without any discernible traces of impurity or secondary phases. Nanoindentation results exhibit discontinuities in the load–displacement curve (so-called multiple "pop-ins" event) during loading, indicating possible involvement of dislocation activities. No discontinuities were observed on unloading segment of the load–displacement curve. Continuous stiffness measurements (CSM) technique was carried out in the nanoindentation tests to determine the hardness and Young's modulus of the hexagonal HMO thin films. The obtained hardness and Young's modulus of the hexagonal HMO thin films are 14.2 ± 0.7 GPa and 219.2 ± 10.6 GPa, respectively with the room-temperature fracture toughness being in the order of 0.4 ± 0.2 MPa $m^{1/2}$.

1. Introduction

Recently, the multiferroic materials with coexisting magnetic and electric orders have received considerable attention [1,2]. This is mostly based on their potential to exhibit "gigantic" magnetoelectric effects enabling the control of magnetization (electric polarization) by an electric (magnetic) field [3], which may lead to new functionalities in the microelectronic devices. The magnetoelectric effect makes the so-called magnetoelectric multiferroics interesting materials for future information-technology devices in which data can be written to magnetic memory elements by applied electric fields. The hexagonal manganites $RMnO_3$ (R = Sc, In, Y, Ho) are one group of magnetoelectric multiferroics. In particular, $HoMnO_3$ (HMO) is a strong magnetoelectric material in the sense that its magnetic phase at low temperature can be controlled by an applied electric field [3]. However, while most of the researches have been concentrated on its magnetoelectric characteristics for device applications, researches on the mechanical properties have not drawn equal attention. Therefore, an accurate measurement of the mechanical properties of hexagonal HMO thin films is required in order to take the full advantage of using them as structural/functional elements in devices.

Nanoindentation technique is especially well suited for characterizing the mechanical characteristics of small structures [4,5] as well as thin films and coatings [6–9]. Analysis of the load–displacement curve obtained by nanoindentation allows the primary parameters such as the hardness and Young's modulus to be obtained without visualizing the indentation. The most adopted method of analysis is the one proposed by Oliver and Pharr [10]. However, in the case of thin films, the response after some penetration depth arises not only from the films but also from the substrate and, the mechanical properties obtained are therefore a combination of both structures. As a result, indentation with contact depths of less than 10% of films thickness is needed to obtain intrinsic film properties and minimize the influence of the substrate [11]. On the other hand, due to the equipment limitations, it is generally very difficult to obtain meaningful analytical results for indentation depths less than 10 nm. Thus, it is almost impossible to obtain substrate independent results for films with thickness thinner than 100 nm. Therefore, in order to get insights on the influence of substrate in a more quantitative manner, especially for thin films, it is essential to monitor the mechanical properties as a function of depth. In this work, we used a dynamic approach, termed as the continuous stiffness measurement (CSM) mode [12], to con-

* Corresponding author. Tel.: +886 7 6577711x3130; fax: +886 7 6578444.
E-mail address: srjian@gmail.com (S.-R. Jian).

0925-8388/$ – see front matter © 2010 Elsevier B.V. All rights reserved.
doi:10.1016/j.jallcom.2010.08.109

tinuously monitor the hardness and Young's modulus values as a function of the indentation depths.

In this study, the structural and mechanical properties of hexagonal HMO thin films were investigated by using the X-ray diffraction (XRD) and nanoindentation techniques. We report, for the first time to our knowledge, the hardness and Young's modulus of hexagonal HMO thin films. In addition, nanoindentation deformation behavior of hexagonal HMO thin films was disclosed by analyzing the nanoindentation load–displacement curves.

2. Experimental details

Sintered ceramic pellet of stoichiometric $HoMnO_3$ was prepared by conventional solid-state reaction method and used as a target for the subsequent pulsed laser deposition (PLD). The PLD process was carried out by using a 248 nm KrF excimer laser operated at a repetition rate of 3 Hz with an energy density of 2–4 J/cm^2. For growing the hexagonal phase HMO films, the (1 1 1)-oriented yttria-stabilized zirconia (YSZ) single crystal was chosen as the substrates. During deposition, the substrate temperature and oxygen pressure were optimized at T_S = 850 °C and $P(O_2)$ = 0.1 Torr, respectively. The film thickness was around 200 nm. High quality epitaxial $HoMnO_3$ (HMO) thin films were obtained under these optimized growth conditions [13]. The film structure was extensively characterized by various X-ray diffraction (XRD) schemes. After that, a Veeco/TM CP-R atomic force microscopy (AFM) was used to measure surface profiles of the samples. For the AFM operation, a constant scan speed of 1 μm/s was used, with a constant load of 30 nN being applied to the cantilever.

The mechanical properties (hardness and Young's modulus) of hexagonal HMO thin films are conducted by using an MTS Nano Indenter® XP instrument with a three-sided pyramidal Berkovich indenter tip. The detailed experimental procedures can be found elsewhere [6–9]. Before applying the loading onto the HMO specimen, nanoindentation must be conducted on the standard sample (here fused silica with Young's modulus of 68–72 GPa was used) to obtain the reasonable loading range. To perform the CSM technique [12], the system was operated by superimposing small oscillations with a frequency of 75 Hz on the force signal to record stiffness data along with load and displacement data dynamically. Firstly, the indenter was loaded and unloaded three times to ensure that the tip was properly in contact with the surface of the materials and that any parasitic phenomenon is released from the measurements. Then, the indenter was loaded for the fourth and final time at a strain rate of 0.05 s^{-1}, with a 60 s holding period inserted at the peak load in order to avoid the influence of creep on unloading characteristics, which were used to compute mechanical properties of the specimen. Furthermore, for the sake of obtaining steady mechanical characteristics and eliminating interference from the environmental fluctuation factor, each indentation test was performed when the thermal drift was below 0.01 nm/s. The analytic method developed by Oliver and Pharr [10] was adopted to determine the hardness and Young's modulus of the hexagonal HMO thin film from the load–displacement curve.

3. Results and discussion

3.1. Structural and surface characteristics

The X-ray diffraction (XRD) θ–2θ pattern for the as-deposited hexagonal HMO thin films grown on (1 1 1)-oriented YSZ substrates is shown in Fig. 1. Only the diffraction peaks corresponding to (0 0 1) family of planes of hexagonal HMO are observed, indicating the formation of a pure hexagonal HMO with the *c*-axis oriented normal to the film surface. The inset of Fig. 1 shows that its full width at half maximum (FWHM) in the rocking curve of the (0 0 4) peak is about 0.49°, which suggests a reasonably good crystalline quality. From the AFM observations (as shown in Fig. 2), the averaged surface roughness of HMO thin film is estimated to be about 0.8 nm. We note that, in addition to the allowable thermal drift for environmental control, sufficiently smooth specimen surface is also a prerequisite for obtaining reliable mechanical characteristics by nanoindentation.

3.2. Nanoindentation results

The results of nanoindentation measurements are displayed in Fig. 3. Fig. 3(a) shows the typical nanoindentation curve obtained for hexagonal HMO thin film. The total penetration depth into thin film was ~55 nm with a peak load of 0.8 mN. The penetration

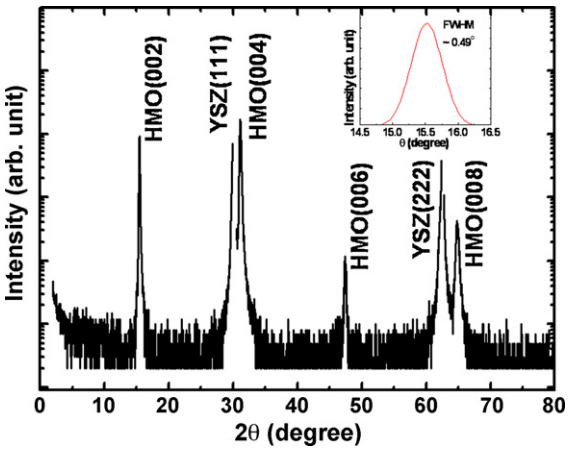

Fig. 1. The θ–2θ X-ray diffractogram of a hexagonal HMO thin film (~200 nm) on YSZ substrate. The inset shows the rocking curve of the (0 0 2) diffraction peak of the HMO film.

dependence of the hardness and Young's modulus of hexagonal HMO thin film calculated from the load–displacement data following the analytical method developed by Oliver and Pharr [10] are shown in Fig. 3(b) and (c), respectively. It can be seen that both the hardness and Young's modulus exhibit a sudden drop around an indentation depth of ~15 nm and remain essentially constant up to ~55 nm, indicating the absence of manifestations from the substrate over this range of indentation depth. This is, in fact, quite consistent with the conclusion drawn by Li et al. [14], wherein they proposed that the nanoindentation depth should never exceed 30% of film thickness.

In Fig. 3(b), the penetration dependent hardness plot can be roughly divided into two stages; namely, the initial increase to a maximum value and the subsequent decrease to a constant value. The increase in hardness at small penetration depth is usually attributed to the transition between purely elastic to elastic/plastic contact whereby the hardness is really the mean contact pressure. Only under the condition of a fully developed plastic zone does the mean contact pressure represent the hardness. When there is no plastic zone, or a partially formed plastic zone, the mean contact

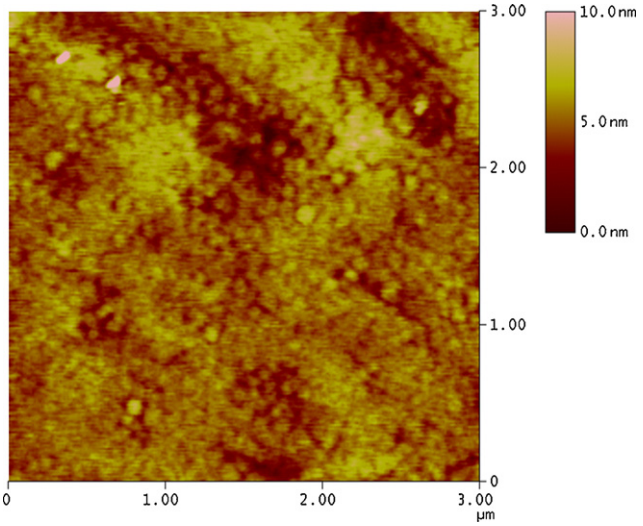

Fig. 2. AFM image of hexagonal HMO thin film deposited on YSZ substrate. The surface roughness of HMO thin film is estimated to be 0.8 nm.

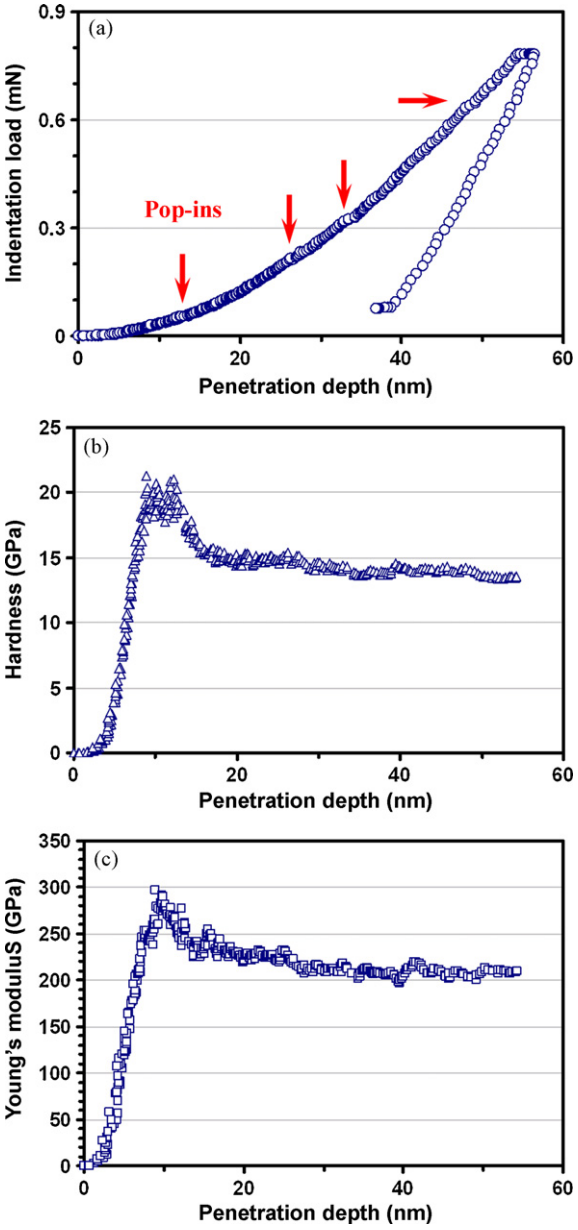

Fig. 3. Nanoindentation measurement results: (a) the load–displacement curve of hexagonal HMO thin film showing the multiple "pop-ins" (arrows) event during loading. Inset: the corresponding SEM nanoindented image; (b) the hardness–displacement curve; and (c) the Young's modulus–displacement curve for the hexagonal HMO thin film.

pressure (which is measured using the Oliver and Pharr method) is less than the nominal hardness. After the first stage, the hardness starts to decrease and reaches a constant value of 14.2 ± 0.7 GPa for hexagonal HMO thin film. The constant characteristic of hardness is consistent with that of a single material; therefore, the hardness values at this stage could be regarded as intrinsic properties of the HMO film. Similarly, the plot of penetration depth dependent Young's modulus of the hexagonal HMO film determined using the method of Oliver and Pharr [10] is plotted in Fig. 3(c). The manifested behaviors, as expected, are akin to those illustrating in Fig. 3(b). The value of Young's modulus for the hexagonal HMO thin film is 219.2 ± 10.6 GPa. Table 1 displays the mechanical properties (hardness and Young's modulus) of HMO thin film and YSZ single crystals for comparison.

Table 1
The mechanical properties of hexagonal HMO thin films and YSZ single crystals.

	Hardness (GPa)	Young's modulus (GPa)
HMO thin film	14.2 ± 0.4[a]	219.2 ± 10.6[a]
YSZ(1 0 0)	12.4 ± 0.4 [15]	237 ± 12 [15]
	16.8 ± 1.8 [16]	281.5 ± 16.0 [16]
YSZ(1 1 0)	18.3 ± 1.8 [16]	257.2 ± 10.2 [16]
YSZ(1 1 1)	19.5 ± 0.6[a]	235.6 ± 5.2[a]
	14.8 ± 0.9 [15]	214 ± 9 [15]
	15.3 ± 1.3 [16]	256.2 ± 13.3 [16]

[a] This present study.

Finally, it is noted that the load–displacement curve displayed in Fig. 3(a) evidently exhibits irregularities, characterized by small sudden displacement excursions (multiple "pop-ins") indicated by the arrows, during loading. The first apparent "pop-in" event occurred at a load about 0.08 mN. Subsequently, the multiple pop-in phenomena are randomly distributed over the entire loading curve. Furthermore, it is interesting to point out that the events of multiple pop-ins are coinciding nicely with sudden decreases in the hardness of measured materials [17]. As can be seen in Fig. 3(b), the hardness of hexagonal HMO thin film decreases abruptly at the penetration depth of ~12 nm corresponding to the first "pop-in" event. After the first pop-in the hardness for the hexagonal HMO film remains essentially constant albeit with the small fluctuations, possibly associated with the dislocation activities.

3.3. Fracture toughness of HMO thin film

In order to delineate the mechanical behaviors in deeper penetration situations, a cyclic load–displacement plot with Berkovich indenter for the hexagonal HMO film is shown in Fig. 4(a). As can be seen in Fig. 4(a), there are no multiple "pop-out" events on the unloading curve. This suggests that phase transitions like that observed in indented Si [9] probably are not occurring in the present case. Moreover, it can be noticed that although only one major subsequent pop-in occurs during the indentation loading curve, there are three obvious cracking events along the corner of residual indentation, as seen in the scanning electron microscopy (SEM) micrograph shown in Fig. 4(b). Therefore, the cause of the subsequent multiple "pop-ins" is attributed to the Berkovich indentation induced cracking on the surface of the hexagonal HMO thin films.

The fracture toughness of brittle materials obtained in indentation measurements can be determined using the following expression [18]:

$$K_{\text{fracture}} = \beta \cdot \left(\frac{E}{H}\right)^{1/2} \cdot \frac{P_{\max}}{c^{3/2}} \quad (1)$$

where β is an empirical constant depending on the geometry of the indenter (0.016 for Berkovich indenter), E is the elastic modulus, H is the hardness, $P_{\max}$ is the peak load of the indentation cycle, and c is the length of the radial crack trace on the material surface after the Berkovich indenter withdrawing. Using the length of the radial crack revealed in the SEM micrograph displayed in Fig. 4(b) which was obtained at a maximum load of 50 mN, one obtains, from Eq. (1), the value of the fracture toughness to be $K_{\text{fracture}} = 0.4 \pm 0.2\ \text{MPa m}^{1/2}$.

3.4. XTEM observations in indented HMO thin film

A bright-field XTEM image of hexagonal HMO thin film after being indented with an indentation load of 50 mN is displayed in Fig. 5. It is evident that there is no sign of delamination in the film/substrate interface, suggesting excellent interfacial bonding between film and substrate. As listed in Table 1, the hardness of

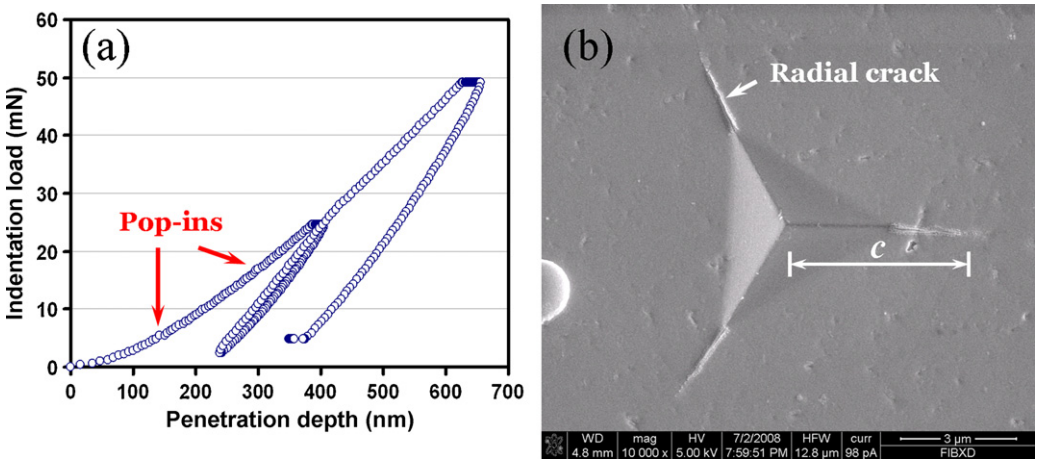

Fig. 4. (a) The typical cyclic load–displacement data for the hexagonal HMO thin film obtained by using a Berkovich indenter showing the multiple "pop-ins"; (b) The SEM micrograph showing the morphology of an indent made after an applied load of 50 mN. Notice the crack formation along the pyramidal edge directions.

HMO thin films is smaller than that of the YSZ substrates. Therefore, the film/substrate structure can be regarded as coating a soft layer on a harder substrate. Upon an applied indentation load of 50 mN, the hexagonal HMO film is subjected to a tremendous compressive plastic strain, resulting in significant bending at the interface. The effects of indentation have, in fact, extended into the YSZ substrate. Consequently, a Berkovich nanoindentation-induced deformed zone is evidently observed in the YSZ substrate, featuring significant dislocation activities seen in Fig. 5.

The multiple "pop-ins" have been reported previously in hexagonal structured sapphire [19], GaN thin films [20–21] and single crystal bulk ZnO [22], while for materials like GaAs and InP with the cubic structure only single "pop-in" event was found [23]. However, different from the spherical tip used in Ref. [23], Jian and Jang [24] proposed that the multiple pop-ins phenomena actually occurred in single crystal InP when a Berkovich indenter tip was used. We suspect that these discrepancies are mainly due to the various indentation methods used. For example, the tip–surface contact configuration and stress distribution for the Berkovich indenter tip can be drastically different from that for the spherical tip. Consequently, the above discussions do suggest that multiple pop-ins indeed are specific features of materials with hexagonal lattice structure and geometry of the indenter tip may play the important roles in determining the nanoindentation-induced mechanical responses.

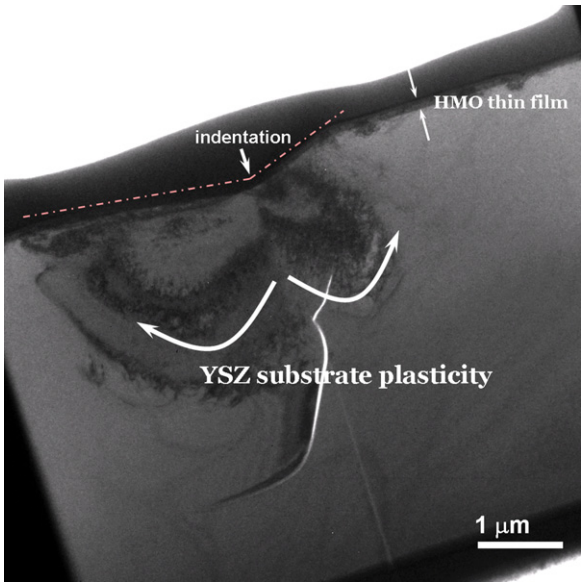

Fig. 5. The bright-field XTEM image in the vicinity immediately under the Berkovich indent applied on the hexagonal HMO thin film with an indentation load of 50 mN.

4. Conclusions

The structural features and nanomechanical properties of the hexagonal (0 0 0 1)-$HoMnO_3$ films deposited on (1 1 1)-YSZ substrates by pulsed laser deposition were systematically studied by using the XRD and nanoindentation techniques. The XRD analysis showed that crystal structure of the obtained HMO films is hexagonal with the *c*-axis perpendicular to the surface of (1 1 1)-YSZ substrate. Nanoindentation results indicated that the values of hardness and Young's modulus of the hexagonal HMO thin film are 14.2 ± 0.7 GPa and 219.2 ± 10.6 GPa, respectively, with the fracture toughness being about 0.4 ± 0.2 MPa $m^{1/2}$.

Acknowledgements

This work was partially supported by the National Science Council of Taiwan, under Grant No.: NSC97-2112-M-214-002-MY2 and NSC99-2112-M-214-001. JYJ is partially supported by the MOE-ATU program operated at NCTU. The technical assistance from Prof. G.J. Chen is gratefully acknowledged.

References

[1] J. Liu, M. Li, L. Pei, J. Wang, B. Yu, X. Wang, X. Zhao, J. Alloys Compd. 493 (2010) 544.
[2] Y.J. Wu, L.H. Tang, H.L. Li, X.M. Chen, J. Alloys Compd. 496 (2010) 269.
[3] T. Lottermoser, T. Lonkai, U. Amann, D. Hohlwein, J. Ihringer, M. Fiebig, Nature 430 (2004) 541.
[4] Y. Raichman, M. Kazakevich, E. Rabkin, Y. Tsur, Adv. Mater. 18 (2006) 2028.
[5] X. Tao, X. Wang, X.D. Li, Nano Lett. 7 (2007) 3172.
[6] S.R. Jian, Nanoscale Res. Lett. 3 (2008) 6.
[7] S.R. Jian, G.J. Chen, T.C. Lin, Nanoscale Res. Lett. 5 (2010) 935.
[8] S.R. Jian, G.J. Chen, J.S.C. Jang, Y.S. Lai, J. Alloys Compd. 494 (2010) 219.
[9] S.R. Jian, G.J. Chen, J.Y. Juang, Curr. Opin. Solid State Mater. Sci. 14 (2010) 69.
[10] W.C. Oliver, G.M. Pharr, J. Mater. Res. 7 (1992) 1564.
[11] T.Y. Tsui, G.M. Pharr, J. Mater. Res. 14 (1999) 292.
[12] X.D. Li, B. Bhushan, Mater. Charact. 48 (2002) 11.
[13] P. Murugavel, J.H. Lee, D. Lee, T.W. Noh, Y. Jo, M.H. Jung, Y.S. Oh, K.H. Kim, Appl. Phys. Lett. 90 (2007) 142902.
[14] X.D. Li, H.S. Gao, C.J. Murphy, L.F. Gou, Nano Lett. 10 (2004) 1903.
[15] K. Kurosaki, D. Setoyama, J. Matsunaga, S. Yamanaka, J. Alloys Compd. 386 (2005) 261.
[16] M. Fujikane, D. Setoyama, S. Nagao, R. Nowak, S. Yamanaka, J. Alloys Compd. 431 (2007) 250.
[17] J.E. Bradby, J.S. Williams, M.V. Swain, J. Mater. Res. 19 (2004) 380.

[18] G.M. Pharr, Mater. Sci. Eng. A 253 (1998) 151.
[19] R. Nowak, T. Sekino, S. Maruno, K. Niihara, Appl. Phys. Lett. 68 (1996) 1063.
[20] S.O. Kucheyev, J.E. Bradby, J.S. Williams, C. Jagadish, M.V. Swain, G. Li, Appl. Phys. Lett. 78 (2001) 156.
[21] C.H. Chien, S.R. Jian, C.T. Wang, J.Y. Juang, J.C. Huang, Y.S. Lai, J. Phys. D: Appl. Phys. 40 (2007) 3985.
[22] S.R. Jian, J. Alloys Compd. 494 (2010) 214.
[23] J.E. Bradby, J.S. Williams, J.W. Leung, M.V. Swain, P. Munroe, Appl. Phys. Lett. 78 (2001) 3235.
[24] S.R. Jian, J.S.C. Jang, J. Alloys Compd. 481 (2009) 498.